Russian Journal of Nonlinear Dynamics, 2018, vol. 14, no. 4, pp. 473–494.
Full-texts are available at http://nd.ics.org.ru
DOI: 10.20537/nd180404

NONLINEAR PHYSICS AND MECHANICS

MSC 2010: 37Mxx, 65Nxx, 70Exx, 76Dxx

Dynamics of a Body with a Sharp Edge in a Viscous Fluid

I. S. Mamaev, V. A. Tenenev, E. V. Vetchanin

This paper addresses the problem of plane-parallel motion of the Zhukovskii foil in a viscous fluid. Various motion regimes of the foil are simulated on the basis of a joint numerical solution of the equations of body motion and the Navier – Stokes equations. According to the results of simulation of longitudinal, transverse and rotational motions, the average drag coefficients and added masses are calculated. The values of added masses agree with the results published previously and obtained within the framework of the model of an ideal fluid. It is shown that between the value of circulation determined from numerical experiments, and that determined according to the model of and ideal fluid, there is a correlation with the coefficient $\mathcal{R} = 0.722$. Approximations for the lift force and the moment of the lift force are constructed depending on the translational and angular velocity of motion of the foil. The equations of motion of the Zhukovskii foil in a viscous fluid are written taking into account the found approximations

Received October 19, 2017
Accepted September 07, 2018

The work of V. A. Tenenev (Sections 2 and Conclusion) was carried out within the framework of the state assignment given to the Izhevsk State Technical University 1.2405.2017/4.6. The work of E. V. Vetchanin (Introduction and Section 1) and I. S. Mamaev (Section 3) was supported by the Russian Foundation for Basic Research under grants Nos. 15-08-09093-a and 18-08-00995-a, respectively.

Ivan S. Mamaev
mamaev@rcd.ru
Institute of Mathematics and Mechanics of the Ural Branch of RAS
ul. S. Kovalevskoi 16, Ekaterinburg, 620990 Russia
Kalashnikov Izhevsk State Technical University
ul. Studencheskaya 7, Izhevsk, 426069 Russia

Valentin A. Tenenev
tenenev@istu.ru
Kalashnikov State Technical University
ul. Studencheskaya 7, Izhevsk, 426069 Russia

Evgeny V. Vetchanin
eugene186@mail.ru
Kalashnikov State Technical University
ul. Studencheskaya 7, Izhevsk, 426069 Russia
Udmurt State University
ul. Universitetskaya 1, Izhevsk, 426034 Russia

and the drag coefficients. The calculation results based on the proposed mathematical model are in qualitative agreement with the results of joint numerical solution of the equations of body motion and the Navier – Stokes equations.

Keywords: Zhukovskii foil, Navier – Stokes equations, joint solution of equations, finite-dimensional model, viscous fluid, circulation, sharp edge

Contents

Introduction

1. The model of an ideal fluid. The simplest and the most widely studied mathematical model describing the motion of a rigid body in an ideal fluid is provided by the Kirchhoff equations [30]. This model takes into account only the resistance of the medium to the accelerated motion of the body (the effect of added masses). At the same time, the body moving uniformly and rectilinearly undergoes no resistance (D'Alembert's paradox). However, this mathematical model gives a qualitative description of the phenomena observed in the dynamics of the free and controlled motion of a rigid body. For example, the authors of [33–35] considered a rigid body moving in an ideal fluid by changing the position of the internal mass. It was shown that the motion of a hydrodynamically asymmetric body is rectilinear if the internal mass moves along a self-intersecting trajectory. In [49], using the results of [33–35], a method was proposed for self-propulsion of an elliptic shell in a fluid by means of two internal eccentrics rotating with angular velocities equal in absolute value and opposite in sign. The results of [49] were experimentally confirmed in [31].

We also mention the works [22, 52] concerned with the dynamics of unbalanced ellipsoidal bodies with internal rotors. In [22], within the framework of the model of an ideal fluid, the controllability of the motion of an unbalanced triaxial ellipsoid by rotating internal rotors is proved, and explicit controls ensuring the rotation of the body about its geometric axes or motion along helical trajectories are presented. It should be noted that the dynamics described in [22] using the model of an ideal fluid differs considerably from that observed in the experiments [54]. In [52], the problem of stabilizing the motion of a balanced ellipsoid by means of rotors is considered.

The development of the model of rigid body motion in an idea fluid involves taking into account the lift force, gravity and interaction with vortices. The expression for the lift force (the

Kutta – Zhukovskii theorem) acting on the foil in a plane-parallel flow was presented in [3, 36] and has the form

$$F = \rho v_\infty \Gamma,$$

where ρ is the density of the medium, v_∞ is the velocity of the unperturbed incoming flow, and Γ is the circulation. For foils with a sharp edge, circulation is defined on the basis of the Kutta – Chaplygin condition [9, 36] so as to ensure finiteness of the velocity on the sharp edge. For smooth bodies, circulation cannot be defined without additional considerations. The authors of [9, 17] obtained expressions for the force and torque (the Chaplygin – Blasius formula) acting on the foil surrounded by a steady-state flow without separation. In the case of nonzero constant circulation, the motion of the body in an ideal fluid is described by the Chaplygin equations, and general expressions for the forces acting in this case on the body are given in [10]. We note that, as in the Chaplygin equations, terms linear in velocities [6] arise in the equations of motion when it comes to describing the three-dimensional motion of nonsimply connected bodies.

Controlled plane-parallel motion with constant circulation by means of a moving internal mass and a rotor was investigated in [50]. In [44], the problem of body motion near a given trajectory by means of a flywheel and piecewise-constant circulation was considered.

Taking into account the gravity force in the equations of motion leads to a qualitative change in the dynamics. In [20], the plane-parallel motion of a smooth foil in an ideal fluid with constant circulation in the gravitational field is considered, a bifurcation analysis of the integrable case of a body with zero buoyancy is carried out, and the onset of chaos in the case of deviation of the system from the state of zero buoyancy is shown. In [2], the motion of a heavy unbalanced ellipsoid in an ideal fluid by means of internal rotors is investigated. Conditions are obtained for unbounded motion and compensation of the drift arising due to the gravity force, under restricted controls. In [18], an analysis is made of the asymptotic behavior and stability of the motion of rigid bodies in an ideal fluid in a gravitational field. In [8], the stability of steady rotations of helical bodies falling in a fluid was investigated. It should be noted that, within the framework of the model of an ideal fluid, these regimes correspond to accelerated motions, which are not observed in experiments.

In most cases, when rigid bodies are surrounded by a flow, vortices arise which change considerably the force action of the fluid. For example, added vortices increase considerably the lift force acting on the Kasper wing [28, 41]. The model of an ideal incompressible fluid does not admit the appearance or disappearance of vortices [5]; however, their existence can be postulated within the framework of a concrete problem. For example, in [24] the lift force is approximately calculated for a delta-shaped wing taking into account vortices formed near edges. The authors replace the original three-dimensional problem with the two-dimensional problem of a segment surrounded by a potential flow with two point vortices situated in the vicinity of edges. The authors of [38] propose the model of rigid body motion with several sharp edges, which takes into account the formation of vortices near edges and the change in their intensity in the process of motion. Based on the mathematical model constructed in [38], the stability of the fall of a flat plate is numerically investigated. It should be noted that the addition of new vortices to the system leads to an increase in the number of dimensions of the phase space. In the case of computer simulation this leads to processor time expenditures increasing in the process of calculation. In [45], the problem of self-propulsion of the Zhukovskii foil by means of oscillations of the rotor and periodic shedding of point vortices is considered. In [45], the intensity of a trailing vortex is calculated using the Kutta – Chaplygin condition; however, in the time intervals between vortex sheddings this condition was violated. In [42, 45],

the results of experimental investigations of controlled motion are presented for foils with a rigid and flexible tail.

2. The model of a viscous fluid. The model of an ideal fluid possesses a number of shortcomings, in particular, the above-mentioned D'Alembert paradox and nonphysical accelerated motions. A description of various paradoxes of the model of an ideal fluid and that of a viscous fluid can be found in [13]. For these reasons it is necessary to take into account viscous friction, which is inevitably present in the observed physical processes. The most complete information on the interaction of the fluid and the body can be obtained from a joint solution of the equations of body motion and the Navier – Stokes equations. When this approach is taken, there is no need for additional assumptions on the magnitude of circulation and vortex shedding.

Controlled motion of rigid nondeformable bodies in a viscous fluid by means of moving internal masses was considered in [43, 51]. In [43, 51], a joint solution of the equations of body motion and the Navier – Stokes equations in velocity – pressure variables was carried out. The plane-parallel motion of a body in a viscous fluid by means of oscillations of the internal mass and by deforming the shell was considered in [25]. For simulation of the fluid flow the authors of [25] used the Navier – Stokes equations in stream function – vorticity variables. The motion of an oscillating elliptic foil and a three-linked body in a viscous fluid was simulated in [26] using the vortex particle method.

The main drawback of the above approach is that the hardware and software must meet high requirements, which makes it unsuitable for parametric investigations in a wide range of parameter values. However, the information obtained from simulation on the basis of the Navier – Stokes equations can be used to construct finite-dimensional models of body motion in a fluid.

The most widespread approach to investigating the motion of rigid bodies in a viscous fluid is to apply finite-dimensional models based on ordinary differential equations. Such models are explored using well-developed analytical and numerical methods for analysis of dynamical systems.

As a rule, when constructing finite-dimensional models one proceeds from the equations of body motion in an ideal fluid, supplementing them with dissipative terms. For example, in describing the motion of heavy plates in a viscous fluid one uses dissipative terms that are either linear [4, 46] or quadratic [11, 12] in velocities. A survey and comparative analysis of various finite-dimensional models of the motion of plates in a fluid is presented in [37]. An example of construction of a finite-dimensional model based on the joint numerical solution of the Navier – Stokes equations and equations of body motion is given in [19]. In [48], a mathematical model of the fall of toroidal bodies in a fluid is constructed using coefficients calculated on the basis of experimental data. The proposed model contains gyroscopic terms describing the influence of the circulating motion of the fluid through a hole in the body, and dissipative terms quadratic in velocities.

We also note that for an approximate description of the motion of rigid bodies in a fluid one can apply nonholonomic models, which, compared to the original mathematical model, have a smaller number of dimensions of the phase space. The approach described above is applicable in the case of a strong anisotropy of the friction coefficients [23, 29, 32]. In [21] it is shown that, as one of the friction coefficients increases indefinitely, the equations of rigid body motion become equations of the Chaplygin sleigh, the controlled motion of which was investigated, for example, in [14–16]. The authors of [53] proposed a more general model, called the hydrodynamical Chaplygin sleigh.

3. Objective of this paper. Finite-dimensional models are constructed to describe the system dynamics for specific parameter values, which makes them unsuitable for analysis of analogous systems with other characteristics. In this paper we pose the problem of constructing

a mathematical model of the motion of the Zhukovskii foil in a viscous fluid. As a basis for construction of equations of motion we use the results obtained within the framework of the model of an ideal fluid and the data of the joint numerical solution of equations of rigid body motion and the Navier – Stokes equations. In Section 1 we describe the main assumptions and present equations describing the joint motion of the body and the fluid. In Section 2 we present the results of numerical simulation of various motion regimes of the Zhukovskii foil. In Section 3 we analyze the forces and the torque acting on the moving foil, and construct finite-dimensional equations of motion.

1. The mathematical model

1.1. Equations of body motion in a viscous fluid

Consider the plane-parallel motion of a homogeneous symmetric foil with a sharp edge in an unbounded mass of an incompressible viscous fluid. Assume that no external forces act on the system of interest. We define the geometry of the foil (see Fig. 1) by applying the Zhukovskii transformation

$$z = \widetilde{x}_1 + i\widetilde{x}_2 = k\left(\zeta + \zeta_c + \frac{1}{\zeta + \zeta_c}\right) \tag{1.1}$$

to the circle $|\zeta| = R_c$. Here $\zeta_c = 1 - R_c$ is the characteristic of the foil and k is the scale factor. The transformation (1.1) is given with respect to the coordinate system $\widetilde{C}\widetilde{x}_1\widetilde{x}_2$ (see Fig. 1). The axis $\widetilde{C}\widetilde{x}_1$ lies on the symmetry line of the foil. The center of mass of the foil lies on the axis $\widetilde{C}\widetilde{x}_1$ and is displaced relative to the origin $\widetilde{C}$.

To describe the motion of the system, we introduce two coordinate systems: a fixed frame Oxy and a moving frame Cx_1x_2 attached to the body (see Fig. 1). The origin C of the moving coordinate system lies at the center of mass of the foil, and the axis Cx_1 lies on the symmetry line of the foil.

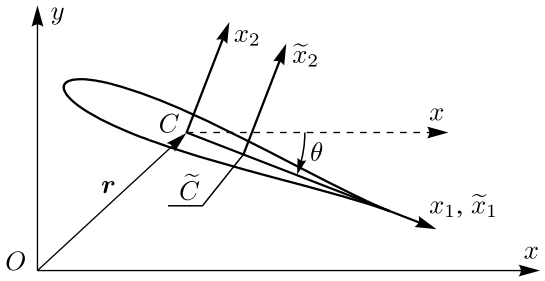

Fig. 1. A fixed coordinate system Oxy and a moving coordinate system Cx_1y_1.

The position of the origin C of the moving coordinate system Cx_1x_2 relative to the fixed coordinate system Oxy will be given by the radius vector $\boldsymbol{r} = (x, y)$, and the orientation, by the angle θ between the positive directions of the axes Ox and Cx_1. Thus, the configuration space of the foil $\mathcal{Q} = \left\{(x,\, y,\, \theta) \mid x,\, y \in \mathbb{R},\ \theta \in \mathbb{S}^1\right\} \approx \mathbb{R}^2 \times \mathbb{S}^1$ coincides with the motion group of the plane $SE(2)$.

The following kinematic relations hold [1]:

$$\dot{x} = v_1 \cos\theta - v_2 \sin\theta, \quad \dot{y} = v_1 \sin\theta + v_2 \cos\theta, \quad \dot{\theta} = \omega, \tag{1.2}$$

where v_1 and v_2 are the projections of the translational velocity of the center of mass of the foil on the axis of the moving coordinate system, and ω is the angular velocity of the foil.

The motion of the foil in a viscous fluid is described by the Newton equations, which have the following form in the moving coordinate system:

$$\dot v_1 = \omega v_2 + f_1, \quad \dot v_2 = -\omega v_1 + f_2, \quad \dot\omega = g. \tag{1.3}$$

Here f_1 and f_2 are the projections of the viscous forces onto the axes of the moving coordinate system, divided by the mass m of the foil, g is the viscous torque divided by the central moment of inertia J of the foil. We note in advance that the values of f_1, f_2, g will be defined on the basis of the numerical solution to the Navier – Stokes equations.

Remark 1. In modeling the motion of a rigid body in a viscous fluid,the authors of [40] defined the forces and torques in the equations of motion on the basis of a numerical solution to the Navier – Stokes equations. In addition, the equations of motion contained terms describing the effect of *added masses*. In order to ascertain the necessity of explicitly taking into account added masses in the equations of motion in the case of their solution jointly with the equations of motion of the fluid, we give a citation from the classical work of L. I. Sedov on the mechanics of continuous media [7, pp. 200–201]:

"In order to solve the problem of the motion of an absolutely rigid body in an unbounded mass of an ideal incompressible fluid, one may apply two methods.

1. Consider the body and the fluid as a single mechanical system with six degrees of freedom. ... Using the formula for the kinetic formula of the system and the information on the elementary work done by the forces external to the body – fluid system and acting on the rigid body (where it is assumed that there are no similar external forces acting on the fluid), one may construct Lagrange's equations of the second kind and with their aid pose and solve different problems. The system of equations thus obtained is analogous to the system of equations of motion for a free rigid body; however, it has a more general form, since the inertia of the body – fluid system is given by the matrix $\|m_{ik} + \lambda_{ik}\|$ which is of a more general nature than the special matrix $\|m_k\|$ for a free rigid body.

2. One can consider from the outset the equations of motion of the rigid body in which one takes into account the resultant force $\boldsymbol{A}$ and the resultant torque $\mathfrak{M}_0$ exerted by the fluid on the body. In this case, one must use the formulae

$$\boldsymbol{A} = \int\limits_\Sigma p\boldsymbol{n}\, d\sigma \quad \text{and} \quad \mathfrak{M}_0 = \int\limits_\Sigma p(\boldsymbol{r}\times\boldsymbol{n})d\sigma,$$

where $\mathfrak{M}_0$ is the moment of the hydrodynamic forces relative to some arbitrary point O fixed in the body...

This method is suitable in cases where the fluid has other boundaries than Σ and where the motion of the fluid *is not potential*..."

Thus, the approach described in [40] appears to be incorrect, and we *do not include the coefficients of added masses in the equations of motion* (1.3) *when they are solved together with the Navier – Stokes equations.*

In the hydrodynamics of an ideal fluid the quantities f_1, f_2 and g which appear in Eqs. (1.3) can be written as

$$f_1 = \frac{-\Gamma v_2 - \lambda_1\dot v_1 + \lambda_2 v_2\omega}{m}, \quad f_2 = \frac{\Gamma v_1 + \lambda_2\dot v_2 - \lambda_1 v_1\omega}{m}, \quad g = \frac{-\lambda_3\dot\omega + (\lambda_1-\lambda_2)\,v_1v_2}{J}, \tag{1.4}$$

where λ_1 and λ_2 are the added masses, λ_3 is the added moment of inertia, and Γ is the circulation whose value, according to the Kutta – Chaplygin condition, is calculated so as to ensure finiteness of the velocity of the fluid on the sharp edge of the foil.

In possible physical processes the magnitude of circulation depends considerably on the regime of motion of the body and cannot be uniquely defined without additional numerical experiments. In view of the above, we formulate the following problems within the framework of the assumptions made in this paper:

– *investigate the degree of agreement of the results of joint numerical solution of the equations of body motion* (1.3) *and the Navier – Stokes equations* (1.6) *with the results obtained within the framework of the model of an ideal fluid*;

– *construct expressions for* f_1, f_2, g *depending on* v_1, v_2, ω, $\dot{v}_1$, $\dot{v}_2$, $\dot{\omega}$ *using the results of numerical simulation and the results obtained within the framework of the model of an ideal fluid.*

1.2. Equations of fluid motion

To define the forces f_1, f_2 and the torque g, which appear in Eq. (1.3), we will numerically solve the Navier – Stokes equations. Since the region occupied by the fluid has a curvilinear boundary determined by the geometry of the foil, it is worthwhile to introduce an orthogonal curvilinear coordinate system (ξ, η) attached to the body, which will allow us to numerically solve the Navier – Stokes equations. We define the coordinate lines $\xi = \text{const}$, $\eta = \text{const}$ as equipotential lines and streamlines of the complex potential

$$\Psi = \xi + i\eta = z\left(\zeta + \frac{R_c^2}{\zeta}\right) \tag{1.5}$$

for the longitudinal flow of an ideal fluid past the foil, the fluid velocity at infinity being unity. Here the function z is defined by the expression (1.1).

Remark 2. We recall that the equations of motion (1.3) are referred to the coordinate system Cx_1x_2. In order to calculate the torque g relative to point C, the computational mesh was constructed taking into account the displacement of the coordinate system Cx_1x_2 relative to $\widetilde{C}\widetilde{x}_1\widetilde{x}_2$.

By defining the levels $\xi = \xi_i$, $i = \overline{1, N_\xi}$, $\eta = \eta_j$, $j = \overline{1, N_\eta}$, we obtain an orthogonal computational mesh. An example of this mesh for a foil with the characteristic $\zeta_c = -0.1$ and the scale factor $k = 0.05$ is shown in Fig. 2.

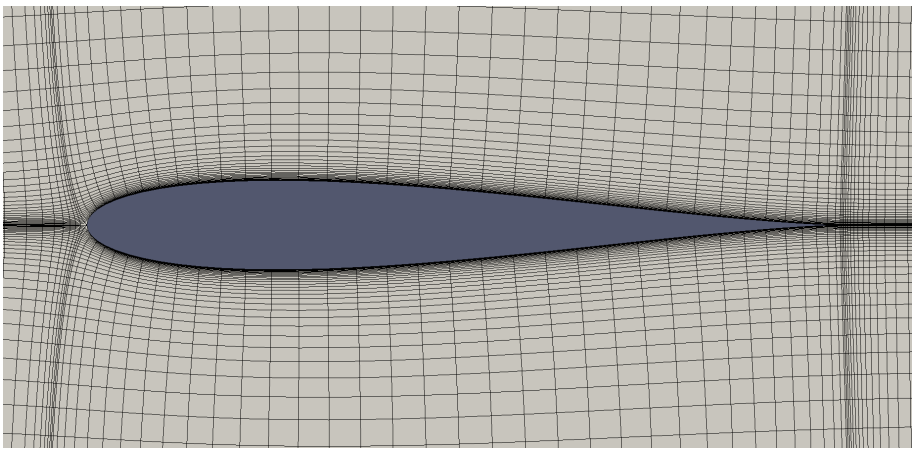

Fig. 2. Computational mesh for a foil with the characteristic $\zeta_c = -0.1$ and the scale factor $k = 0.05$.

The Navier – Stokes equations in a curvilinear coordinate system take the following form:

$$\frac{\partial Du_1}{\partial \xi}+\frac{\partial Du_2}{\partial \eta}=0,$$

$$\frac{\partial u_1}{\partial t}+\frac{1}{D^2}\left(\frac{\partial D(u_1-w_1)u_1}{\partial \xi}+\frac{\partial D(u_2-w_2)u_1}{\partial \eta}\right)=-\frac{1}{D\rho_f}\frac{\partial p}{\partial \xi}+\frac{\nu}{D^2}\left(\frac{\partial^2 u_1}{\partial \xi^2}+\frac{\partial^2 u_1}{\partial \eta^2}\right)+B_1, \quad (1.6)$$

$$\frac{\partial u_2}{\partial t}+\frac{1}{D^2}\left(\frac{\partial D(u_1-w_1)u_2}{\partial \xi}+\frac{\partial D(u_2-w_2)u_2}{\partial \eta}\right)=-\frac{1}{D\rho_f}\frac{\partial p}{\partial \eta}+\frac{\nu}{D^2}\left(\frac{\partial^2 u_2}{\partial \xi^2}+\frac{\partial^2 u_2}{\partial \eta^2}\right)+B_2,$$

$$B_1=\frac{1}{D^2}\left((u_2-w_2)u_2\frac{\partial D}{\partial \xi}-(u_1-w_1)u_2\frac{\partial D}{\partial \eta}+u_2\omega D^2\right)+$$
$$+\frac{\nu}{D^3}\left(-(u_1-w_1)\left(\frac{\partial^2 D}{\partial \xi^2}+\frac{\partial^2 D}{\partial \eta^2}\right)-2\frac{\partial u_2}{\partial \eta}\frac{\partial D}{\partial \xi}+2\frac{\partial u_2}{\partial \xi}\frac{\partial D}{\partial \eta}\right),$$

$$B_2=\frac{1}{D^2}\left((u_1-w_1)u_1\frac{\partial D}{\partial \eta}-(u_2-w_2)u_1\frac{\partial D}{\partial \xi}-u_1\omega D^2\right)+$$
$$+\frac{\nu}{D^3}\left(-(u_2-w_2)\left(\frac{\partial^2 D}{\partial \xi^2}+\frac{\partial^2 D}{\partial \eta^2}\right)+2\frac{\partial u_1}{\partial \eta}\frac{\partial D}{\partial \xi}-2\frac{\partial u_1}{\partial \xi}\frac{\partial D}{\partial \eta}\right),$$

where u_1 and u_2 are the projections of the absolute velocity of the fluid onto the curvilinear axes, w_1 and w_2 are the projections of the transport velocity onto the curvilinear axes, p is the pressure, ρ_f is the density of the fluid, and ν is the kinematic viscosity. Since the mesh was constructed using analytical functions, the Lamé coefficients are the same by virtue of the Cauchy – Riemann conditions and are $D=\sqrt{\left(\frac{\partial x_1}{\partial \xi}\right)^2+\left(\frac{\partial x_2}{\partial \xi}\right)^2}$. The components w_1 and w_2 of the transport velocity vector are calculated by the following formulae:

$$w_1=\frac{1}{D}\left(\frac{\partial x_1}{\partial \xi}(v_1-x_2\omega)+\frac{\partial x_2}{\partial \xi}(v_2+x_1\omega)\right),$$
$$w_2=\frac{1}{D}\left(-\frac{\partial x_2}{\partial \xi}(v_1-x_2\omega)+\frac{\partial x_1}{\partial \xi}(v_2+x_1\omega)\right). \quad (1.7)$$

On the boundary of the foil S, the kinematic boundary conditions were given by

$$u_1\Big|_S=w_1\Big|_S, \quad u_2\Big|_S=w_2\Big|_S,$$

and the pressure on the external boundary Σ of the computational region was given by

$$p\Big|_\Sigma=p_0.$$

The finite-volume method of numerical integration of Eqs. (1.6) is described in [39, 43]. The method of joint solution of (1.6) and (1.3) is described in [40]. For the closure of the system of linear algebraic equations obtained in discretizing equations (1.6), the following boundary conditions were additionally postulated:

$$\frac{\partial p}{\partial \boldsymbol{n}}\Big|_S=0, \quad \frac{\partial u_1}{\partial \boldsymbol{n}}\Big|_\Sigma=\frac{\partial u_2}{\partial \boldsymbol{n}}\Big|_\Sigma=0,$$

where $\boldsymbol{n}$ is the unit normal vector to the boundary S or Σ.

The projections of the viscous forces, f_1 and f_2, and the viscous torque, g, were defined using the following loop integrals:

$$f_1 = \frac{1}{m}\int\limits_S \left(p\frac{\partial x_2}{\partial \xi} + \frac{\rho_f \nu}{D}\frac{\partial u_1}{\partial \eta}\frac{\partial x_1}{\partial \xi}\right) d\xi,$$
$$f_2 = \frac{1}{m}\int\limits_S \left(-p\frac{\partial x_1}{\partial \xi} + \frac{\rho_f \nu}{D}\frac{\partial u_1}{\partial \eta}\frac{\partial x_2}{\partial \xi}\right) d\xi, \tag{1.8}$$
$$g = \frac{1}{J}\int\limits_S \left(x_1\left(-p\frac{\partial x_1}{\partial \xi} + \frac{\rho_f \nu}{D}\frac{\partial u_1}{\partial \eta}\frac{\partial x_2}{\partial \xi}\right) - x_2\left(p\frac{\partial x_2}{\partial \xi} + \frac{\rho_f \nu}{D}\frac{\partial u_1}{\partial \eta}\frac{\partial x_1}{\partial \xi}\right)\right) d\xi.$$

2. Numerical analysis of different regimes of motion of the foil

2.1. Parameter values and the scheme of numerical experiments

Consider the motion of the foil for the following parameter values:

- scale factor $k = 0.05$;
- characteristic of the foil $\zeta_c = -0.1$;
- density of the fluid and density of the material of the foil $\rho_f = \rho_b = 1000$ kg/m^3;
- kinematic viscosity $\nu = 10^{-6}$ m^2/s.

For the above parameter values the foil possesses the following mass-geometric characteristics:

- length of the foil ≈ 0.202 m;
- width of the foil ≈ 0.0238 m;
- mass of the foil $m \approx 2.904$ kg;
- central moment of inertia $J \approx 0.0056$ kg $\cdot$ m^2.

The forces f_1, f_2 and the torque g by which the fluid acts on the foil depend greatly on the regime of its motion. To investigate this dependence, we divide the process of motion of the foil into three stages:

1. Motion uniformly accelerated from rest for 0.1 s to given values of velocities v_1^*, v_2^*, ω^*. At this stage of motion, the influence of viscous forces turns out to be insignificant, and the force action of the fluid will be determined predominantly by pressure distribution along the contour of the foil (the effect of added masses).
2. Uniform motion with velocities v_1^*, v_2^*, ω^* for 0.1 s. This stage is transitional and is required for the damping of perturbations arising in the fluid due to a transition from the accelerated motion of the foil to uniform motion.
3. Inertial motion under the action of viscous forces and torque. At this stage, the fluid flow pattern and the regime of motion of the body will undergo considerable changes, leading to changes in the circulation.

Below we will consider separately the longitudinal, transverse and rotational motion of the foil. Based on the first stage of the corresponding numerical experiments, we will calculate the coefficients of added masses. Based on the results of the second and third stages, we will determine the average values of the drag coefficients.

We will also consider the mixed regime of motion for different $v_1^* \in [-2, 0]$ m/s, $v_2^* \in [0, 1]$ m/s, $\omega^* \in [0, 2]$ s^{-1}. Based on the results of the second and third stages of simulation of the mixed regime of motion, we will define the dependence of circulation on v_2 and ω.

2.2. Translational motion in the longitudinal and transverse directions and rotational motion

1. Motion in the longitudinal direction. Consider the motion regime corresponding to $v_1^* = -1$ m/s, $v_2^* = 0$ m/s, $\omega^* = 0$ s^{-1}. In this case, the flow past the foil occurs without separation of the boundary layer, and a viscous wake is formed behind the body. The flow pattern in the case of longitudinal motion is similar to that shown in Fig. 7.

At the first stage, the foil moves with acceleration $a_1 = 10$ m/s^2, and the value of the longitudinal force divided by the mass is $f_1 = 1.32$. Consequently, the added mass corresponding to the longitudinal motion can be approximated by the following expression:

$$\lambda_1 = 0.132m. \tag{2.1}$$

The formula (2.1) agrees with the results of [27] obtained within the framework of the model of an ideal fluid:

$$\lambda_1 = m\left(R_c^2 - 2 + \frac{R_c^2}{(R_c^2-\zeta_c^2)^2}\right)\Big/ R_c^2\left(1 - \frac{1}{(R_c^2-\zeta_c^2)^2}\right) \approx 0.136m. \tag{2.2}$$

According to the results of simulation of the motion of the foil at the second and third stages, the following dependence was obtained for f_1:

$$f_1 = -C_1 v_1|v_1|, \quad C_1 = 1.05. \tag{2.3}$$

The expression (2.3) describes the data of numerical simulation with the correlation coefficient $\mathcal{R} = 0.902$,[1] which is indicative of a sufficiently good agreement between the calculated data and the approximation (2.3).

In the case of longitudinal motion, the transverse force divided by the mass, f_2, and the torque divided by the moment of inertia, g, are close to zero.

2. Motion in the transverse direction. Consider the regime of motion corresponding to $v_1^* = 0$ m/s, $v_2^* = 1$ m/s, $\omega^* = 0$ s^{-1}. In this case, the flow of the fluid is characterized by the presence of two added vortices near the sharp edge and the frontal part of the foil on the leeward side (see Fig. 3). The intensity of the vortices increases with the passage of time.

The motion of the foil at the first stage occurs with acceleration $a_2 = 10$ m/s^2, and the added mass can be approximated by the following expression:

$$\lambda_2 = 11.07m. \tag{2.4}$$

The formula (2.4) agrees with the results of [27]:

$$\lambda_2 = m\left(R_c^2 + 2 + \frac{R_c^2}{(R_c^2-\zeta_c^2)^2}\right)\Big/ R_c^2\left(1 - \frac{1}{(R_c^2-\zeta_c^2)^2}\right) = 10.96m. \tag{2.5}$$

[1] We recall that the correlation of two quantities x and y is calculated as follows: $\mathcal{R} = \dfrac{\sum_{i=1}^N (x_i - \overline{x})(y_i - \overline{y})}{\sqrt{\sum_{i=1}^N (x_i - \overline{x})^2 (y_i - \overline{y})^2}}$, where $\overline{x}$ and $\overline{y}$ are the average values of x and y, respectively [47]. The value $|\mathcal{R}| \in [0.7, 1]$ is indicative of a sufficiently strong relation between the two random variables.

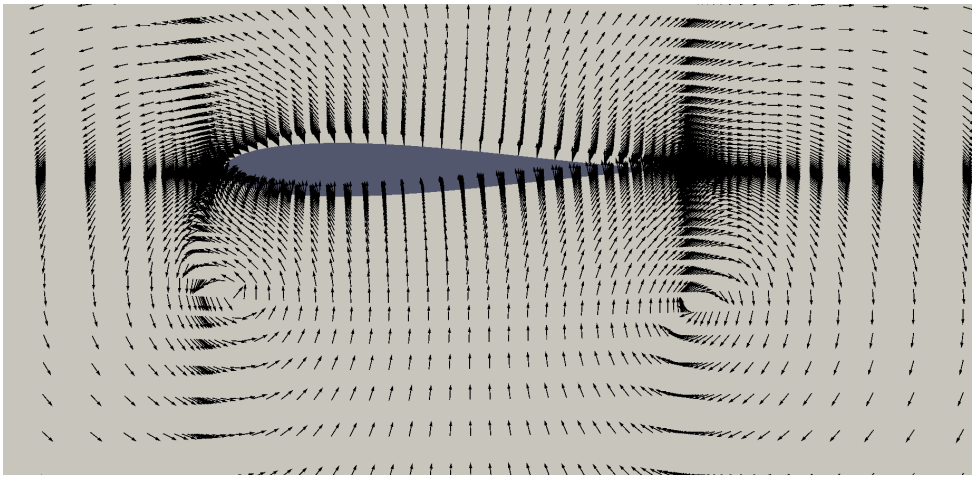

Fig. 3. The velocity field corresponding to the transverse motion for $t = 0.2$ s.

According to the results of motion simulation at the second and third stages, the following dependence was obtained for f_2:

$$f_2 = -C_2 v_2 |v_2|, \quad C_2 = 81.4. \tag{2.6}$$

The expression (2.6) describes the data of numerical simulation with the correlation coefficient $\mathcal{R} = 0.994$, which is indicative of a very good agreement between the calculated data and the approximation (2.6).

3. Rotational motion. Consider the motion regime corresponding to $v_1^* = v_2^* = 0$ m/s, $\omega^* = 2$ s^{-1}. In this case, two vortices arise on opposite sides of the foil near its frontal part and the sharp edge (see Fig. 4).

At the first stage, the foil moves with the angular acceleration $\varepsilon = 2$ s^{-2}, and the added moment of inertia can be approximated as follows:

$$\lambda_3 = 7.21J. \tag{2.7}$$

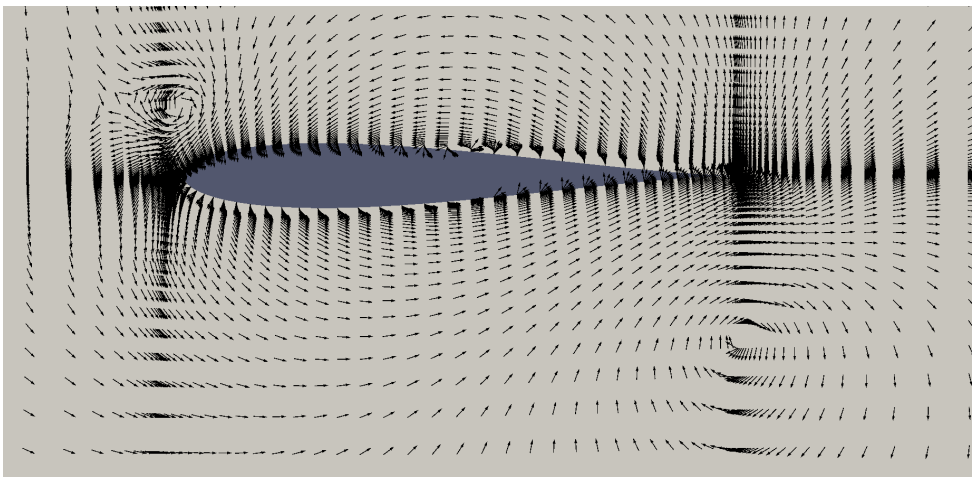

Fig. 4. The velocity field corresponding to the rotational motion for $t = 0.225$ s.

The expression (2.7) agrees well with the results of [27]:

$$\lambda_3 = J\frac{\pi}{160}\left(2 + R_c^2\zeta_c^2 + 2\zeta_c^2 - \frac{2\zeta_c^2}{R_c^2-\zeta_c^2} + \frac{2\zeta_c^2}{(R_c^2-\zeta_c^2)^2} + \frac{R_c^2\zeta_c^2}{(R_c^2-\zeta_c^2)^4}\right) = 7.13J. \tag{2.8}$$

At the second and third stages of motion, the following dependence was obtained for g:

$$g = -C_3\omega|\omega|, \quad C_3 = 28.5. \tag{2.9}$$

The expression (2.9) approximates the data of numerical simulation with the coefficient of determination $\mathcal{R} = 0.974$, which is indicative of a very good agreement between the calculated data and the approximation (2.9).

In conclusion of this subsection, we note that the agreement between the expressions (2.1), (2.4), (2.7) and the results of [27] confirms what is stated in Remark 1.

2.3. The mixed regime

Consider the motion regime corresponding to $v_1^* = -1$ m/s, $v_2^* = 0.5$ m/s, $\omega^* = 2$ s^{-1}. Figures 5–7 show the velocity field in a neighborhood of the foil at times $t = 0.202$ s, $t = 0.225$ s, $t = 0.3$ s.

Figures 5 and 6 show that, at the beginning of the third stage of motion, vortices are formed on the stern. However, after a rather short transient regime (Fig. 7), vortex-free flow sets in around the foil. Separations of vortices lead to oscillations of the transverse force and torque (see Fig. 8). The values of the force and torque become close to zero after completion of the transient process and establishment of the flow without separation.

Thus, *when the inertial motion of the Zhukovskii foil under the action of viscous forces and torque is simulated, the influence of vortex structures is considerable only during a short transient process. For this reason, when constructing the finite-dimensional model of uncontrolled motion, we do not neglect the influence of vortices.*

3. Construction of the finite-dimensional model

3.1. Numerical analysis of forces and torques acting on the body

When constructing the finite-dimensional model of the motion of the Zhukovskii foil in a viscous fluid, we will use as a basis the results obtained within the framework of the theory of an ideal fluid. It is well known that in the presence of circulation Γ the contour is acted upon by the additional Zhukovskii force applied at the conformal center of gravity $\boldsymbol{r}_0 = (x_0, y_0)$ and proportional to the velocity $\boldsymbol{v}_0$ of this point [5]:

$$\boldsymbol{F}_{ideal} = i\rho_f\Gamma\boldsymbol{v}_0, \quad \boldsymbol{v}_0 = \dot{\boldsymbol{r}}_0, \quad \boldsymbol{r}_0 = \int_L z d\varphi, \tag{3.1}$$

where $\varphi = \arg z$.

The complex potential of the flow generated by the moving foil is described by the following expression [27]:

$$\Phi = v_1\Phi_1 + v_2\Phi_2 + \omega\Phi_3 + \Gamma\Phi_4, \tag{3.2}$$

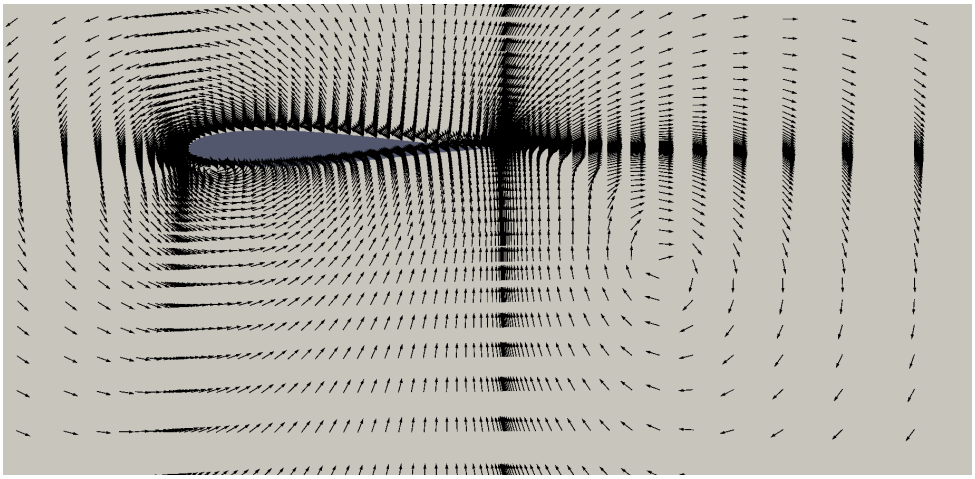

Fig. 5. The velocity field at time $t = 0.202$ s.

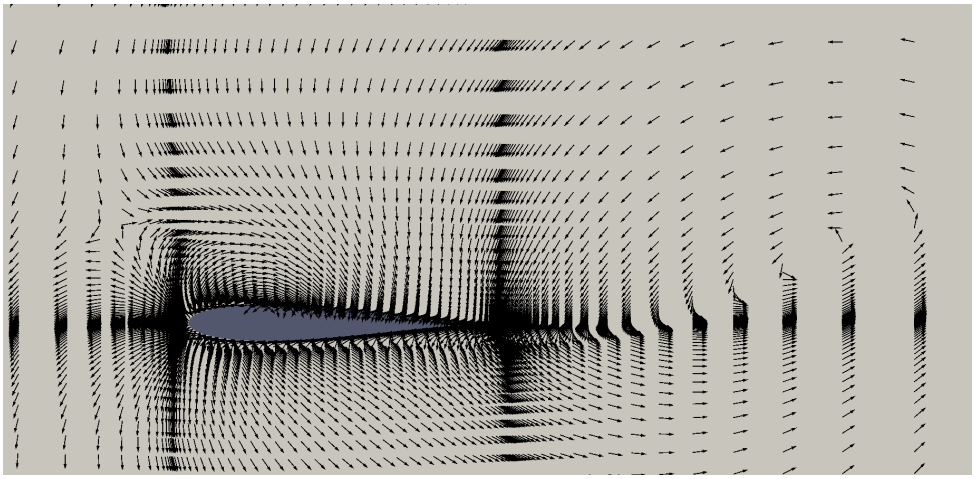

Fig. 6. The velocity field at time $t = 0.225$ s.

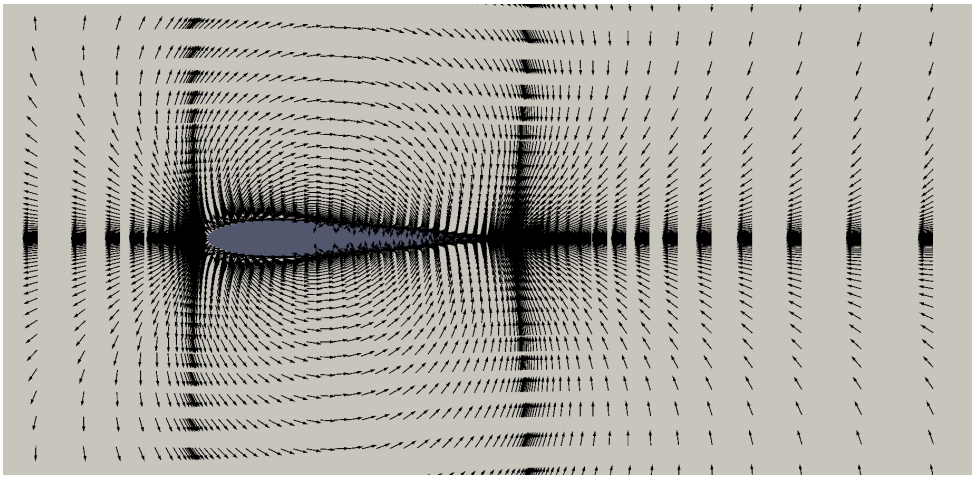

Fig. 7. The velocity field at time $t = 0.3$ s.

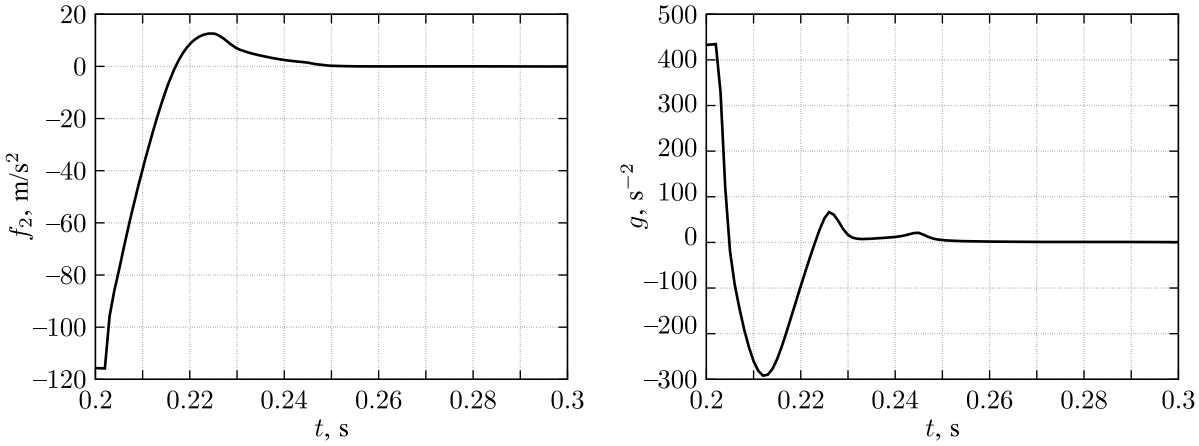

Fig. 8. Change transversely to the force f_2 (divided by the mass) and the torque g (divided by the moment of inertia).

$$\Phi_1 = k\left(-\frac{R_c^2}{\zeta} + \zeta_c + \frac{1}{\zeta+\zeta_c}\right), \quad \Phi_2 = k\left(\frac{R_c^2}{\zeta} + \zeta_c + \frac{1}{\zeta+\zeta_c}\right),$$

$$\Phi_3 = -\frac{ik^2}{2}\left(R_c^2 + \zeta_c^2 + 2\zeta_c\frac{R_c^2}{\zeta} + 2\frac{R_c^2 + \zeta\overline{\zeta}_c}{\zeta(\zeta+\zeta_c)} + \frac{\zeta-\zeta_c}{(\zeta+\zeta_c)(R_c^2-\zeta_c^2)}\right),$$

$$\Phi_4 = \frac{1}{2\pi i}\ln\frac{\zeta}{\zeta_c}.$$

To define circulation Γ, we apply the Kutta–Chaplygin condition to the potential (3.2). According to this condition, circulation must ensure that the complex velocity is zero $\left(\dfrac{d\Phi}{d\zeta} = 0\right)$ at the critical point $\zeta = 1 - \zeta_c$. In this case,

$$\Gamma = 2\pi k(1-\zeta_c)(2v_2 + \beta\omega), \quad \beta = k(2+\zeta_c). \tag{3.3}$$

1. We show that, as the foil moves in the viscous fluid, the sharp edge has a considerable influence on the magnitude of circulation. Figure 9 compares the values of circulation obtained in the numerical experiments and on the basis of the formula (3.3), for different values of v_2 and ω.

We describe the method of constructing Fig. 9. Suppose that at time t_i the transverse component of the velocity of the body is $v_2(t_i)$ and the angular velocity is $\omega(t_i)$. According to the results of the numerical experiments, we calculate circulation $\Gamma_c(t_i)$ by using the integration of vorticity within the limits of 40 mesh layers adjoining the foil. We calculate the value of circulation $\Gamma(t_i)$ by the formula (3.3). Let us plot the point $(\Gamma(t_i), \Gamma_c(t_i))$ on the plane (Γ, Γ_c). Repeating the described actions for subsequent instants of time, we obtain Fig. 9.

Using the least square technique, we construct the linear approximation (see Fig. 9)

$$\Gamma_c = 0.435\Gamma + 0.037.$$

Between the values of Γ and Γ_c there is a correlation with the correlation coefficient 0.722. *The rather high value of the coefficient of correlation of* Γ *and* Γ_c *is indicative of a significant influence of the sharp edge on the flow of the viscous fluid and hence on the magnitude of circulation.*

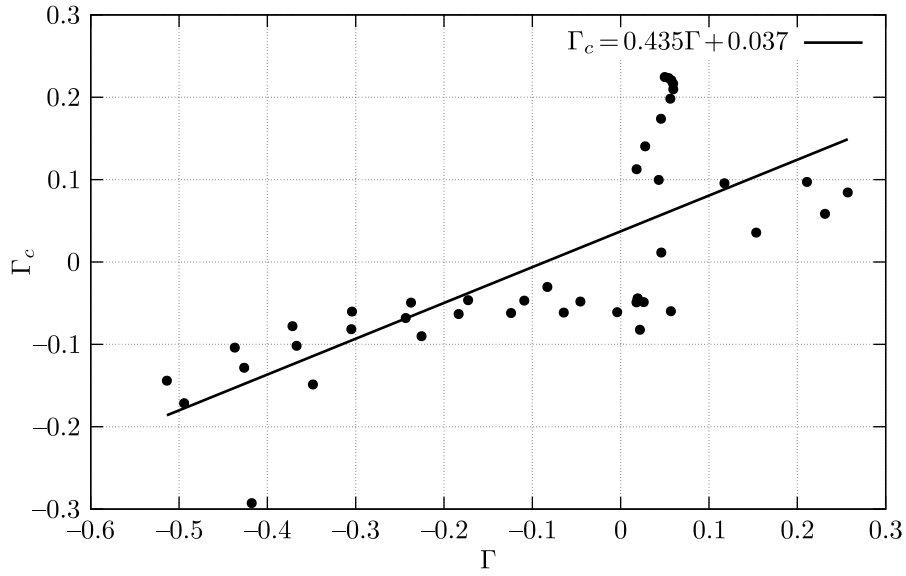

Fig. 9. Comparison of the values of circulation Γ and Γ_c.

2. To define the transverse force component due to circulation, we compare the values of the lift force obtained by the formulae (3.1)

$$f_{2,ideal} = \frac{\rho_f \Gamma v_1}{m} \tag{3.4}$$

with the results of the numerical experiments. To define the contribution of circulation, we exclude from consideration the contribution of frontal resistance and the effect of added masses:

$$f_{2,\Gamma} = f_2 - C_2 v_2 |v_2| - \frac{\lambda_2 \dot{v}_2}{m}. \tag{3.5}$$

The markers in Fig. 10 denote points corresponding to the values of $f_{2,ideal}$ and $f_{2,\Gamma}$, which are reached at equal values of the velocities.

Using the results presented in Fig. 10, the following approximation was constructed for the transverse component of the lift force:

$$f_{2,\Gamma} = 0.983 f_{2,ideal}. \tag{3.6}$$

Between the values of $f_{2,\Gamma}$ and $f_{2,ideal}$ there is a correlation with the coefficient $\mathcal{R} = 0.960$. This ensures a good approximation of the transverse component of the lift force by the expression (3.6), which we write in the explicit form

$$f_{2,\Gamma} = 0.983 \frac{\rho_f \Gamma v_1}{m}, \tag{3.7}$$

where Γ is calculated according to (3.3).

3. According to (3.1), the longitudinal component of the lift force is defined by the expression

$$f_{1,ideal} = -\frac{\rho_f \Gamma (v_2 - x_0 \omega)}{m}. \tag{3.8}$$

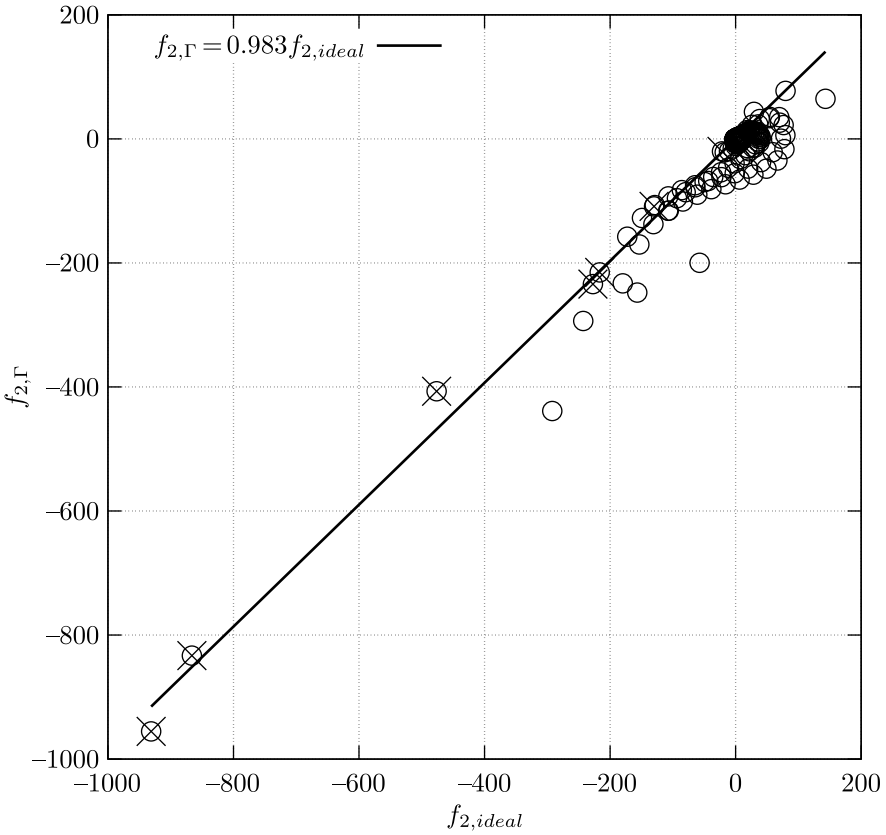

Fig. 10. Comparison of values of the lift force $f_{2,\Gamma}$ obtained in the numerical experiments and $f_{2,ideal}$ obtained by the formula (3.4). The points denoted by the round marker correspond to the third stage, and those denoted by the crossed-out marker correspond to the second stage.

To calculate the contribution of circulation to the longitudinal component of the lift force, we exclude the contribution of the frontal resistance and the effect of added masses:

$$f_{1,\Gamma} = f_1 - C_1 v_1 |v_1| - \frac{\lambda_1 \dot{v}_1}{m}. \tag{3.9}$$

The markers in Fig. 11 denote points corresponding to the values of $f_{1,\Gamma}$ and $f_{1,ideal}$, which have been calculated for equal values of the velocities v_1, v_2, ω.

Using the results presented in Fig. 11, the following approximation was constructed for the longitudinal component of the lift force:

$$f_{1,\Gamma} = 0.0665 f_{1,ideal}. \tag{3.10}$$

Between the values of $f_{1,\Gamma}$ and $f_{1,ideal}$ there is a correlation with the coefficient $\mathcal{R} = 0.848$.

Thus, the longitudinal component of the lift force for the motion of the Zhukovskii foil in a viscous fluid can be approximated by the expression

$$f_{1,\Gamma} = -0.0665 \frac{\rho_f \Gamma (v_2 - x_0 \omega)}{m}. \tag{3.11}$$

We recall that here x_0 is the coordinate of the conformal center of gravity and Γ is calculated by the formula (3.3).

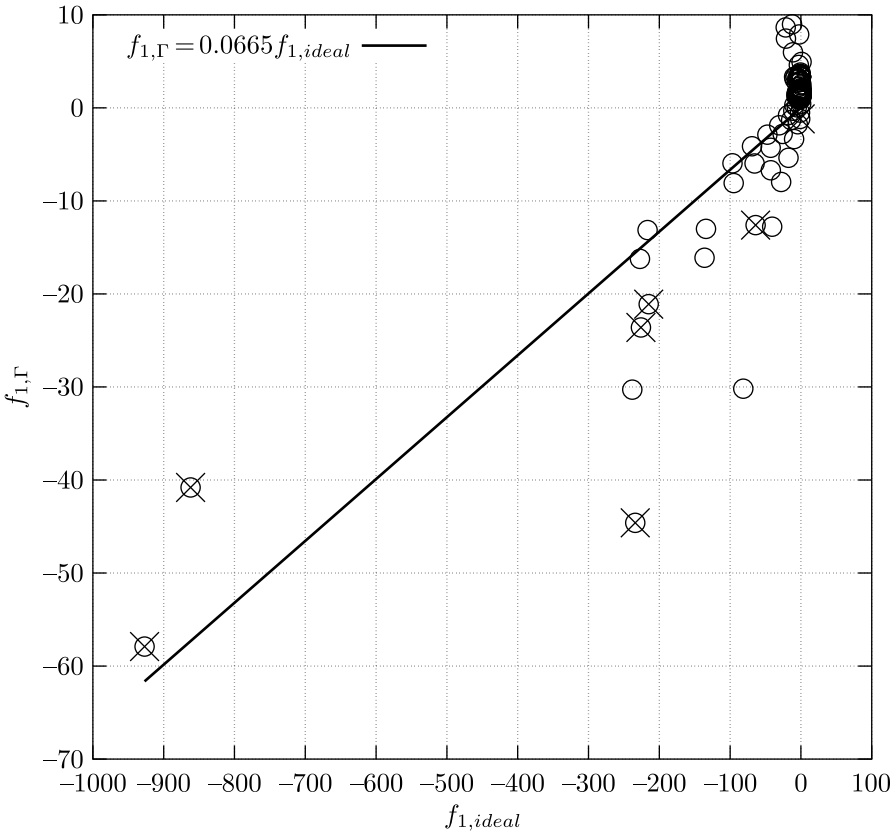

Fig. 11. Comparison of values of the lift force $f_{1,\Gamma}$ obtained in the numerical experiments, and $f_{1,ideal}$ obtained by the formula (3.8). The points denoted by the round marker correspond to the third stage, and those denoted by the crossed-out marker correspond to the second stage.

Remark 3. For commensurable values of the velocities v_1 and v_2 the force components $f_{1,ideal}$ and $f_{2,ideal}$, calculated by the formulae (3.8) and (3.4), respectively, have equal orders, while the forces $f_{1,\Gamma}$ and $f_{2,\Gamma}$ corresponding to the viscous flow differ by more than an order. This difference in the values of $f_{1,\Gamma}$ and $f_{2,\Gamma}$ is due to the nature of the forces. The main contribution to the transverse force f_2 is made by the integration of pressure along the contour, with

$$\left| \int p \frac{\partial x_1}{\partial \xi} \, d\xi \right| \gg \left| \int \frac{\rho_f \nu}{D} \frac{\partial v_1}{\partial \eta} \frac{\partial x_2}{\partial \xi} \, d\xi \right|. \tag{3.12}$$

At the same time, the component from the pressure difference in the longitudinal direction is commensurable with the contribution of the tangential friction stress and is much smaller than the component from the pressure difference in the transverse direction

$$\left| \int p \frac{\partial x_2}{\partial \xi} \, d\xi \right| \ll \left| \int p \frac{\partial x_1}{\partial \xi} \, d\xi \right|. \tag{3.13}$$

4. To calculate the torque acting on the foil, it is necessary to define the point of application Δ of the resultant force. The change in the value of Δ in time is shown in Fig. 12 for the values $v_1^* = -1$ m/s, $v_2^* = 0.5$ m/s, $\omega^* = 2$ s^{-1}.

Figure 12 shows that the position of the point of application of the force is not constant. The processing of the dependence $g = \Delta \cdot f_2$ for several v_1^*, v_2^*, ω^* gives the value of $\Delta \approx 0.005$. Thus, the lift-force moment can be approximated by the expression

$$g_\Gamma = \Delta \cdot f_{2,\Gamma}. \tag{3.14}$$

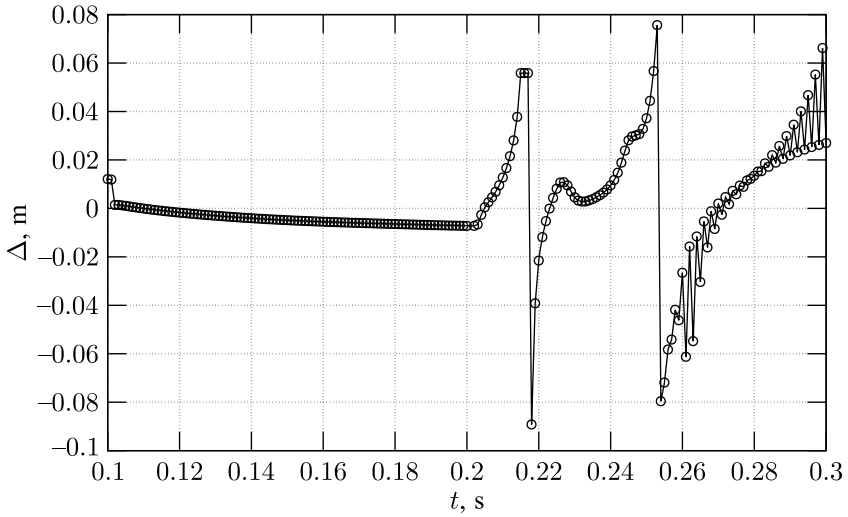

Fig. 12. Time dependence of the point of application of the resultant force.

3.2. The finite-dimensional model

The equations of motion of the Zhukovskii foil in a viscous fluid with the approximation (2.3), (2.6), (2.9), (3.7), (3.11), (3.14) taken into account can be written as

$$\dot v_1 = \omega v_2 - \frac{a_1\rho_f\Gamma}{m}(v_2 - x_0\omega) - C_1 v_1|v_1|, \quad \dot v_2 = -\omega v_1 + \frac{a_2\rho_f\Gamma}{m}v_1 - C_2 v_2|v_2|,$$
$$\dot\omega = \frac{a_2\rho_f\Delta\Gamma}{J}v_1 - C_3\omega|\omega| \tag{3.15}$$

where $a_1 = 0.0665$, $a_2 = 0.983$, $C_1 = 1.05$, $C_2 = 81.4$, $C_3 = 28.5$, $\Delta = 0.005$, and Γ is calculated by the formula (3.3).

Remark 4. The linear and angular accelerations that arose in the numerical experiments were insignificant. For this reason we do not include the coefficients of added masses in Eqs. (3.15). Therefore, the use of Eqs. (3.15) for simulation of the controlled motion of the Zhukovskii foil can lead to incorrect results.

Equations (3.15) differ from the corresponding equations obtained within the framework of the model of an ideal fluid in that they have correction coefficients a_1, a_2 and dissipative terms $C_1 v_1|v_1|$, $C_2 v_2|v_2|$, $C_3\omega|\omega|$.

Consider the motion of the system (3.15) at the third stage with the initial conditions $v_1(0) = -1$, $v_2(0) = 0.5$, $\omega(0) = 2$. Figure 13 shows the time dependences $v_1(t)$, $v_2(t)$ and $\omega(t)$ obtained on the basis of Eqs. (3.15) and the joint solution of Eqs. (1.3) and (1.6).

It can be seen from Fig. 13 that the curves $v_1(t)$, $v_2(t)$ and $\omega(t)$ obtained on the basis of the joint solution of Eqs. (1.3) and (1.6) have pronounced extrema in the initial interval. This is due to the fact that the joint solution of Eqs. (1.3) and (1.6) takes into account the transient process, which is accompanied by the formation and separation of vortices. After completion of this transient process the solution of Eqs. (3.15) agrees with the solution of Eqs. (1.3) and (1.6) both qualitatively and quantitatively.

The trajectory of the foil for the case considered is shown in Fig. 14.

It is seen from Fig. 14 that the motions of the foil calculated on the basis of the model (1.2), (3.15) and Eqs. (1.2), (1.3), (1.6) are in general in qualitative agreement with each other.

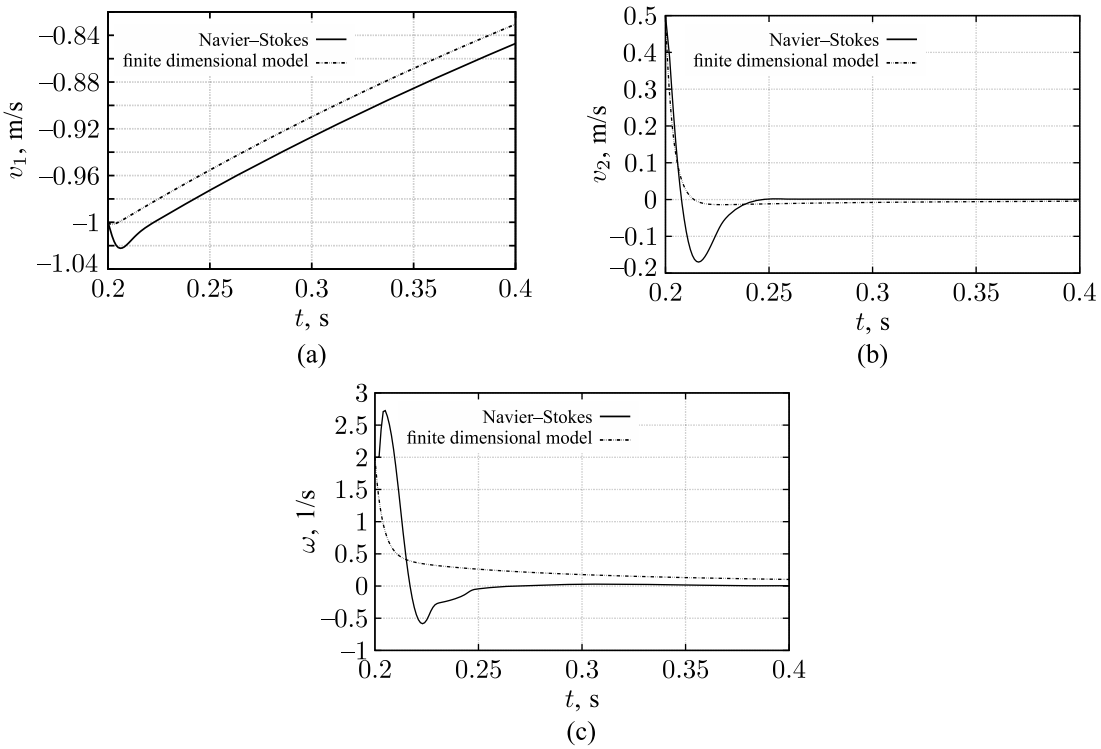

Fig. 13. Dependences: a) $v_1(t)$, b) $v_2(t)$, c) $\omega(t)$, obtained within the framework of the model (3.15) and on the basis of the joint solution of Eqs. (1.3) and (1.6)

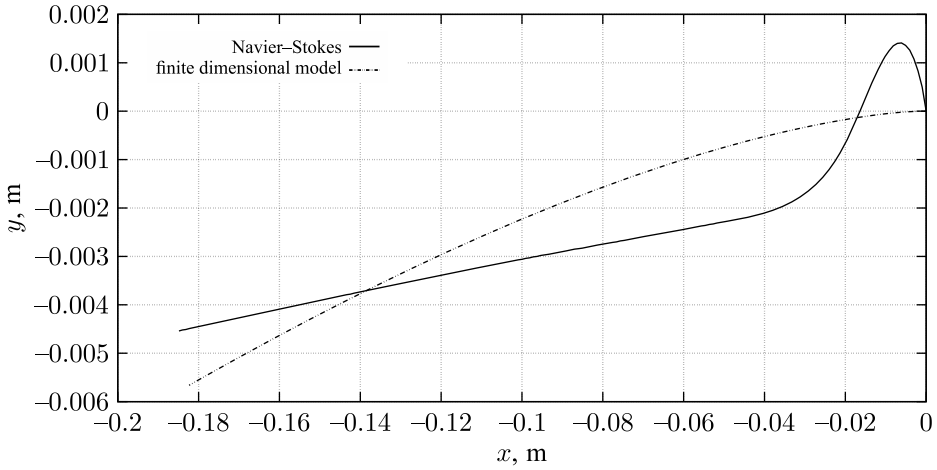

Fig. 14. Trajectory of the center of mass.

The greatest difference is observed in the initial segment, which corresponds to separation of the vortices.

Thus, *in general, Eqs.* (3.15) *qualitatively describe the uncontrolled motion of the Zhukovskii foil in a viscous fluid. To simulate the controlled motion of the foil, it is necessary to define more precisely Eqs.* (3.15) *with the aid of additional numerical experiments.*

Acknowledgments. The authors express their appreciation to A. V. Borisov for the formulation of the problem and valuable comments.

References

[1] Borisov, A. V. and Mamaev, I. S., *Rigid Body Dynamics: Hamiltonian Methods, Integrability, Chaos,* Izhevsk: R&C Dynamics, Institute of Computer Science, 2005 (Russian).

[2] Vetchanin, E. V. and Kilin, A. A., Control of the Motion of an Unbalanced Heavy Ellipsoid in an Ideal Fluid Using Rotors, *Nelin. Dinam.,* 2016, vol. 12, no. 4, pp. 663–674 (Russian).

[3] Zhukovsky, N. E., *Collected Works: Vol. 1,* Moscow: Gostekhizdat, 1937 (Russian).

[4] Kozlov, V. V., On the Problem of Fall of a Rigid Body in a Resisting Medium, *Mosc. Univ. Mech. Bull.,* 1990, vol. 45, no. 1, pp. 30–36; see also: *Vestn. Mosk. Univ. Ser. 1. Mat. Mekh.,* 1990, no. 1, pp. 79–86.

[5] Kochin, N. E., Kibel, I. A., and Roze, N. V., *Theoretical Hydrodynamics,* New York: Wiley, 1964.

[6] Lamb, H., *Hydrodynamics,* 6th ed., New York: Dover, 1945.

[7] Sedov, L. I., *A Course in Continuum Mechanics: Vol. 2. Physical Functions and Formulations of Problems,* Groningen: Wolters-Noordhoff, 1972.

[8] Tenenev, V. A., Vetchanin, E. V., Ilaletdinov, L. F., Chaotic Dynamics in the Problem of the Fall of a Screw-Shaped Body in a Fluid, *Nelin. Dinam.,* 2016, vol. 12, no. 1, pp. 99–120 (Russian).

[9] Chaplygin, S. A., On the Pressure Exerted by a Plane-Parallel Flow upon an Obstructing Body (Contribution to the Theory of Aircraft), in *The Selected Works on Wing Theory of Sergei A. Chaplygin,* San Francisco: Garbell Research Foundation, 1956, pp. 1–16; see also: *Mat. Sb.,* 1910, vol. 28, no. 1, pp. 120–166.

[10] Chaplygin, S. A., On the Action of a Plane-Parallel Air Flow upon a Cylindrical Wing Moving within It, in *The Selected Works on Wing Theory of Sergei A. Chaplygin,* San Francisco: Garbell Research Foundation, 1956, pp. 42–72.

[11] Andersen, A., Pesavento, U., and Wang, Z. J., Analysis of Transitions between Fluttering, Tumbling and Steady Descent of Falling Cards, *J. Fluid Mech.,* 2005, vol. 541, pp. 91–104.

[12] Belmonte, A., Eisenberg, H., and Moses, E., From Flutter to Tumble: Inertial Drag and Froude Similarity in Falling Paper, *Phys. Rev. Lett.,* 1998, vol. 81, no. 2, pp. 345–348.

[13] Birkhoff, G., *Hydrodynamics: A Study in Logic, Fact, and Similitude,* Princeton: Princeton Univ. Press, 2015.

[14] Bizyaev, I. A., Borisov, A. V., Kozlov, V. V., and Mamaev, I. S., Fermi-Like Acceleration and Power Law Energy Growth in Nonholonomic Systems, arXiv:1807.06262 (2018).

[15] Bizyaev, I. A., Borisov, A. V., and Kuznetsov, S. P., The Chaplygin Sleigh with Friction Moving due to Periodic Oscillations of an Internal Mass, arXiv:1807.06340 (2018).

[16] Bizyaev, I. A., Borisov, A. V., and Mamaev, I. S., The Chaplygin Sleigh with Parametric Excitation: Chaotic Dynamics and Nonholonomic Acceleration, *Regul. Chaotic Dyn.,* 2017, vol. 22, no. 8, pp. 955–975.

[17] Blasius, H., Funktionentheoretische Methoden in der Hydrodynamik, *Z. Math. Phys.,* 1910, vol. 58, pp. 90–110.

[18] Borisov, A. V., Kozlov, V. V., and Mamaev, I. S., Asymptotic Stability and Associated Problems of Dynamics of Falling Rigid Body, *Regul. Chaotic Dyn.,* 2007, vol. 12, no. 5, pp. 531–565.

[19] Borisov, A. V., Kuznetsov, S. P., Mamaev, I. S., and Tenenev, V. A., Describing the Motion of a Body with an Elliptical Cross Section in a Viscous Uncompressible Fluid by Model Equations Reconstructed from Data Processing, *Tech. Phys. Lett.,* 2016, vol. 42, no. 9, pp. 886–890; see also: *Pis'ma Zh. Tekh. Fiz.,* 2016, vol. 42, no. 17, pp. 9–19.

[20] Borisov, A. V. and Mamaev, I. S., On the Motion of a Heavy Rigid Body in an Ideal Fluid with Circulation, *Chaos,* 2006, vol. 16, no. 1, 013118, 7 pp.

[21] Borisov, A. V., Mamaev, I. S., and Vetchanin, E. V., Dynamics of a Smooth Profile in a Medium with Friction in the Presence of Parametric Excitation, *Regul. Chaotic Dyn.,* 2018, vol. 23, no. 4, pp. 480–502.

[22] Borisov, A. V., Vetchanin, E. V., and Kilin, A. A., Control Using Rotors of the Motion of a Triaxial Ellipsoid in a Fluid, *Math. Notes,* 2017, vol. 102, nos. 3–4, pp. 455–464; see also: *Mat. Zametki,* 2017, vol. 102, no. 4, pp. 503–513.

[23] Brendelev, V. N., On the Realization of Constraints in Nonholonomic Mechanics, *J. Appl. Math. Mech.,* 1981, vol. 45, no. 3, pp. 351–355; see also: *Prikl. Mat. Mekh.,* 1981, vol. 45, no. 3, pp. 481–487.

[24] Brown, C. E. and Michael, W. H., Effect of Leading-Edge Separation on the Lift of a Delta Wing, *J. Aeronaut. Sci.,* 1954, vol. 21, no. 10, pp. 690–694.

[25] Childress, S., Spagnolie, S. E., and Tokieda, T., A Bug on a Raft: Recoil Locomotion in a Viscous Fluid, *J. Fluid Mech.,* 2011, vol. 669, pp. 527–556.

[26] Eldredge, J. D., Numerical Simulation of the Fluid Dynamics of $2D$ Rigid Body Motion with the Vortex Particle Method, *J. Comput. Phys.,* 2007, vol. 221, no. 2, pp. 626–648.

[27] Mason, R. J., Fluid Locomotion and Trajectory Planning for Shape-Changing Robots, *PhD Dissertation,* Pasadena, Calif.: California Institute of Technology, 2003, 264 pp.

[28] Kasper, W., Aircraft Wing with Vortex Generation, U.S. Patent No. 3 831 885 (27 Aug 1974).

[29] Karapetyan, A. V., On Realizing Nonholonomic Constraints by Viscous Friction Forces and Celtic Stones Stability, *J. Appl. Math. Mech.,* 1981, vol. 45, no. 1, pp. 30–36; see also: *Prikl. Mat. Mekh.,* 1981, vol. 45, no. 1, pp. 42–51.

[30] Kirchhoff, G., *Vorlesungen über mathematische Physik: Vol. 1. Mechanik,* Leipzig: Teubner, 1876.

[31] Klenov, A. I. and Kilin, A. A., Influence of Vortex Structures on the Controlled Motion of an Above-Water Screwless Robot, *Regul. Chaotic Dyn.,* 2016, vol. 21, nos. 7–8, pp. 927–938.

[32] Kozlov, V. V., Realization of Nonintegrable Constraints in Classical Mechanics, *Sov. Phys. Dokl.,* 1983, vol. 28, pp. 735–737; see also: *Dokl. Akad. Nauk SSSR,* 1983, vol. 272, no. 3, pp. 550–554.

[33] Kozlov, V. V. and Ramodanov, S. M., The Motion of a Variable Body in an Ideal Fluid, *J. Appl. Math. Mech.,* 2001, vol. 65, no. 4, pp. 579–587; see also: *Prikl. Mat. Mekh.,* 2001, vol. 65, no. 4, pp. 592–601.

[34] Kozlov, V. V. and Ramodanov, S. M., On the Motion of a Body with a Rigid Hull and Changing Geometry of Masses in an Ideal Fluid, *Dokl. Phys.,* 2002, vol. 47, no. 2, pp. 132–135; see also: *Dokl. Akad. Nauk,* 2002, vol. 382, no. 4, pp. 478–481.

[35] Kozlov, V. V. and Onishchenko, D. A., Motion of a Body with Undeformable Shell and Variable Mass Geometry in an Unbounded Perfect Fluid: Special Issue Dedicated to Victor A. Pliss on the Occasion of His 70th Birthday, *J. Dynam. Differential Equations,* 2003, vol. 15, nos. 2–3, pp. 553–570.

[36] Kutta, W. M., Auftriebskräfte in strömenden Flüssigkeiten, *Illustr. aeronaut. Mitteilungen,* 1902, vol. 6, pp. 133–135.

[37] Kuznetsov, S. P., Plate Falling in a Fluid: Regular and Chaotic Dynamics of Finite-Dimensional Models, *Regul. Chaotic Dyn.,* 2015, vol. 20, no. 3, pp. 345–382.

[38] Michelin, S. and Llewellyn Smith, S. G., An Unsteady Point Vortex Method for Coupled Fluid-Solid Problems, *Theor. Comput. Fluid Dyn.,* 2009, vol. 23, no. 2, pp. 127–153.

[39] Mittal, R., Dong, H., Bozkurttas, M., Najjar, F. M., Vargas, A., and von Loebbecke, A., A Versatile Sharp Interface Immersed Boundary Method for Incompressible Flows with Complex Boundaries, *J. Comput. Phys.,* 2008, vol. 227, no. 10, pp. 4825–4852.

[40] Mougin, G. and Magnaudet, J., The Generalized Kirchhoff Equations and Their Application to the Interaction between a Rigid Body and an Arbitrary Time-Dependent Viscous Flow, *Int. J. Multiph. Flow,* 2002, vol. 28, no. 11, pp. 1837–1851.

[41] Nelson, R., Protas, B., and Sakajo, T., Linear Feedback Stabilization of Point-Vortex Equilibria near a Kasper Wing, *J. Fluid Mech.,* 2017, vol. 827, pp. 121–154.

[42] Pollard, B., Berkey, T., and Tallapragada, Ph., Direct Tail Actuation vs Internal Rotor Propulsion in Aquatic Robots, in *ASME 2017 Dynamic Systems and Control Conference (Tysons, Va., USA, Oct 11–13, 2017): Vol. 1,* Paper No. DSCC2017-5208, V001T30A008, 6 pp.

[43] Ramodanov, S. M. and Tenenev, V. A., Motion of a Body with Variable Distribution of Mass in a Boundless Viscous Liquid, *Nelin. Dinam.,* 2011, vol. 7, no. 3, pp. 635–647 (Russian).

[44] Ramodanov, S. M., Tenenev, V. A., and Treschev, D. V., Self-Propulsion of a Body with Rigid Surface and Variable Coefficient of Lift in a Perfect Fluid, *Regul. Chaotic Dyn.,* 2012, vol. 17, no. 6, pp. 547–558.

[45] Tallapragada, Ph., A Swimming Robot with an Internal Rotor As a Nonholonomic System, in *Proc. of the American Control Conference (Chicago, Ill., USA, July 1–3, 2015),* pp. 657–662.

[46] Tanabe, Y. and Kaneko, K., Behavior of a Falling Paper, *Phys. Rev. Lett.,* 1994, vol. 73, no. 10, pp. 1372–1375.

[47] van der Waerden, B. L., *Mathematische Statistik,* 3rd ed., Grundlehren Math. Wiss., vol. 87, Berlin: Springer, 2012.

[48] Vetchanin, E. V. and Gladkov, E. S., Identification of Parameters of the Model of Toroidal Body Motion Using Experimental Data, *Nelin. Dinam.,* 2018, vol. 14, no. 1, pp. 99–121 (Russian).

[49] Vetchanin, E. V. and Kilin, A. A., Controlled Motion of a Rigid Body with Internal Mechanisms in an Ideal Incompressible Fluid, *Proc. Steklov Inst. Math.,* 2016, vol. 295, pp. 302–332; see also: *Tr. Mat. Inst. Steklova,* 2016, vol. 295, pp. 321–351.

[50] Vetchanin, E. V. and Kilin, A. A., Control of Body Motion in an Ideal Fluid Using the Internal Mass and the Rotor in the Presence of Circulation around the Body, *J. Dyn. Control Syst.,* 2017, vol. 23, no. 2, pp. 435–458.

[51] Vetchanin, E. V., Mamaev, I. S., and Tenenev, V. A., The Self-Propulsion of a Body with Moving Internal Masses in a Viscous Fluid, *Regul. Chaotic Dyn.,* 2013, vol. 18, nos. 1–2, pp. 100–117.

[52] Woolsey, C. A. and Leonard, N. E., Underwater Vehicle Stabilization by Internal Rotors, in *Proc. of the American Control Conference (San Diego, Calif., 1999),* pp. 3417–3421.

[53] Fedorov, Yu. N. and García-Naranjo, L. C., The Hydrodynamic Chaplygin Sleigh, *J. Phys. A,* 2010, vol. 43, no. 43, 434013, 18 pp.

[54] Karavaev, Yu. L., Kilin, A. A., and Klekovkin, A. V., Experimental Investigations of the Controlled Motion of a Screwless Underwater Robot, *Regul. Chaotic Dyn.,* 2016, vol. 21, nos. 7–8, pp. 918–926.